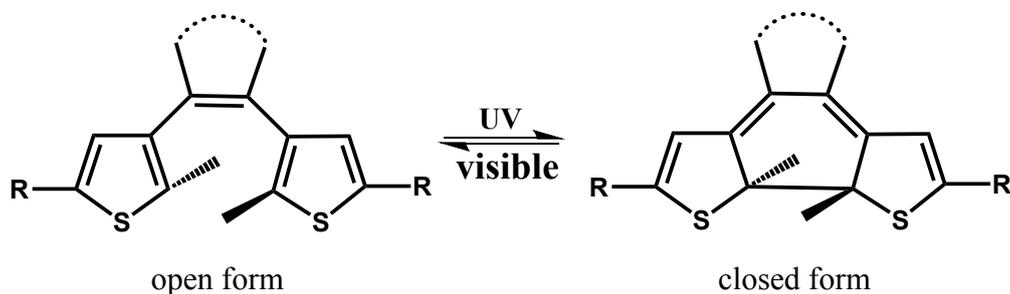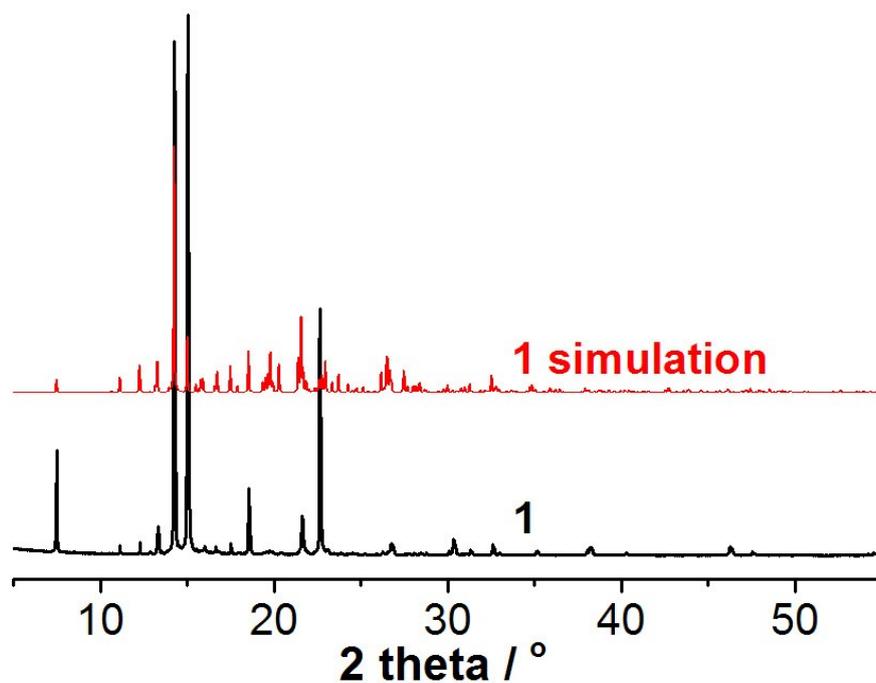# Electronic Supporting Information

Scheme S1 Photochromic interconversion of a BTE unit

Table S1 Solid-state emission data of **1** and **2** before and after irradiation with 365 nm light at room temperature

Compound	λ_{max} (nm)
1	433, 448, 482, 531, 570
1 after irradiation	428, 447, 482, 531
2	460, 489, 535, 593
2 after irradiation	460, 486, 535

Fig. S1 Experimental and simulated XRD patterns of **1**

1

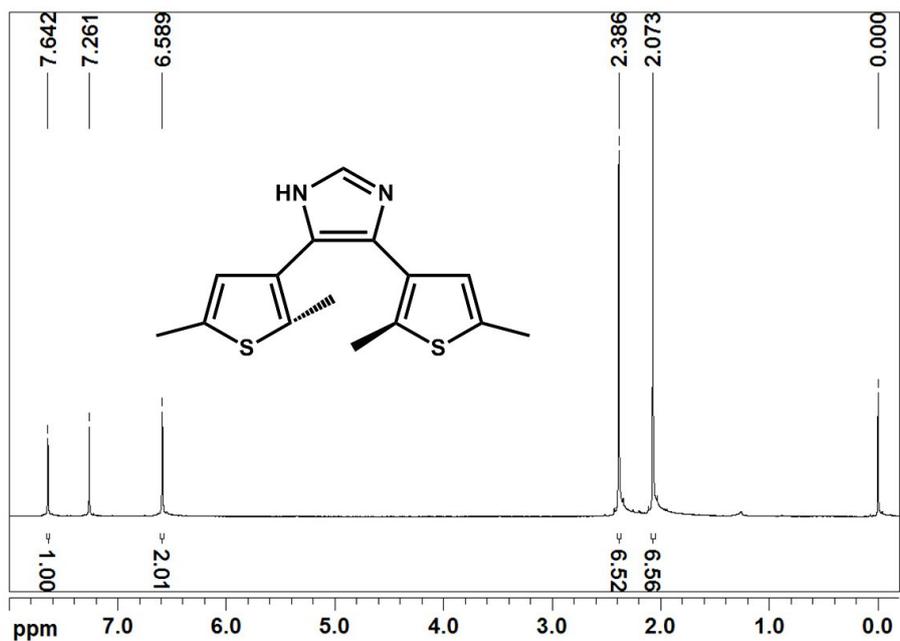**Fig. S2** ^1H NMR spectrum of **1** (500 MHz, CDCl₃).
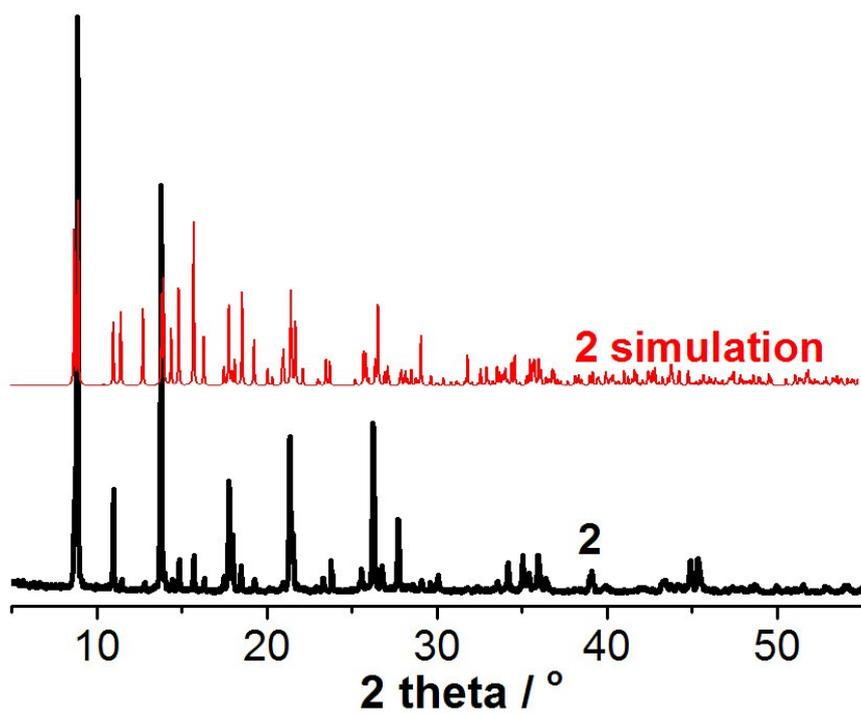

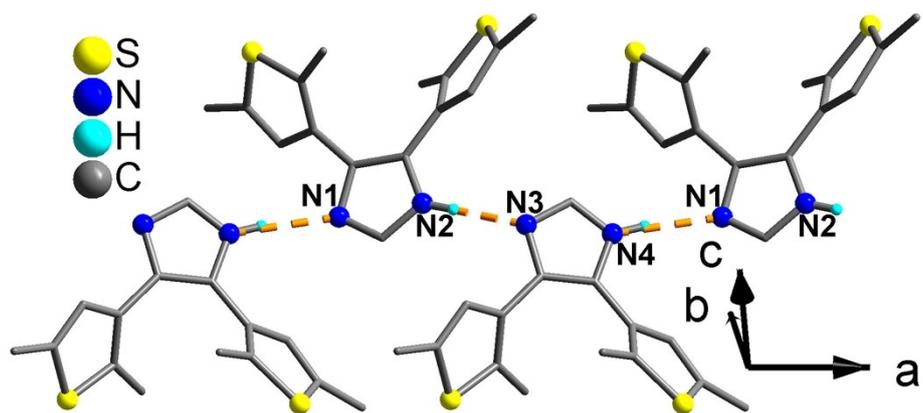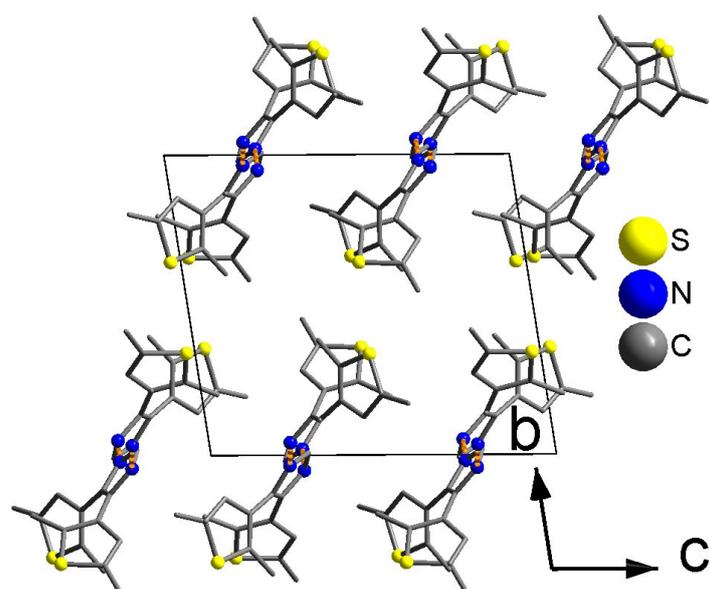**Fig. S3** Experimental and simulated XRD patterns of **2**.

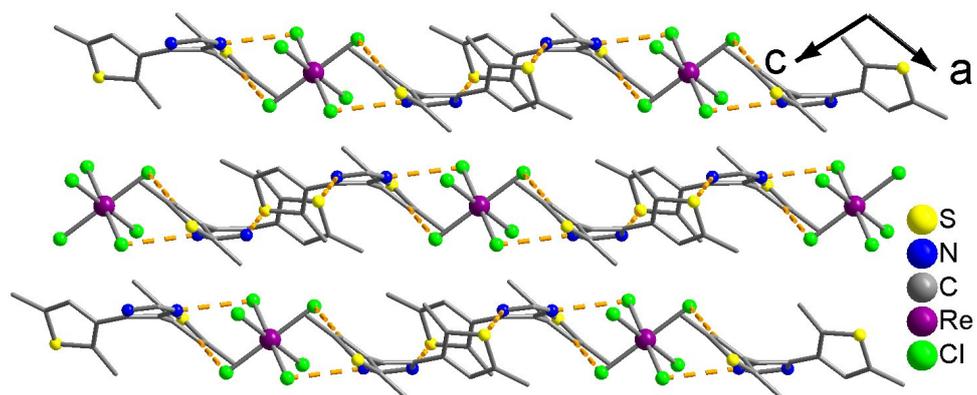**Fig. S4** The supramolecular chain structure in **1**.
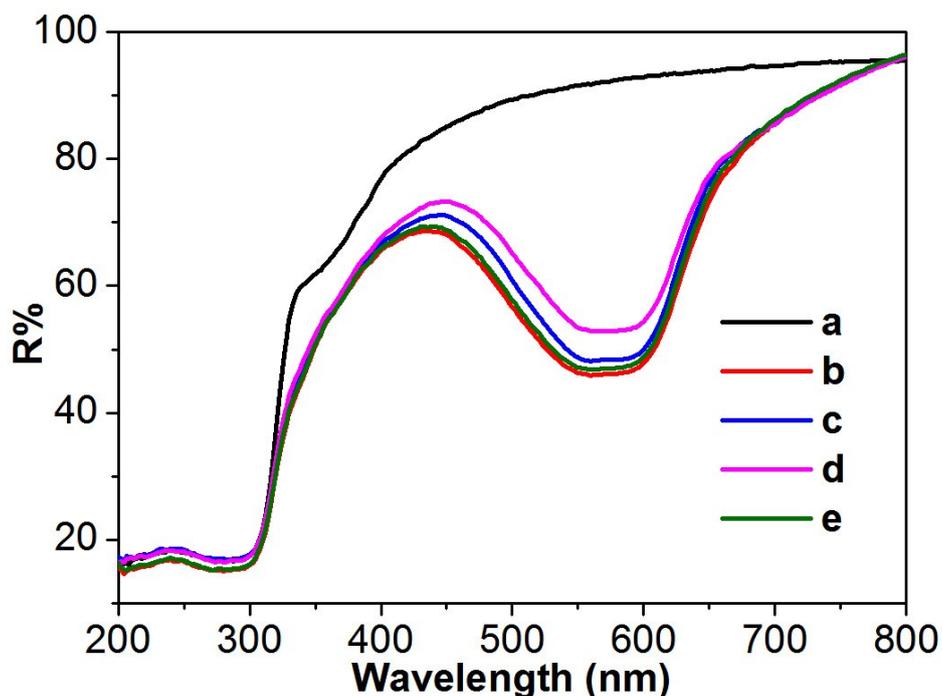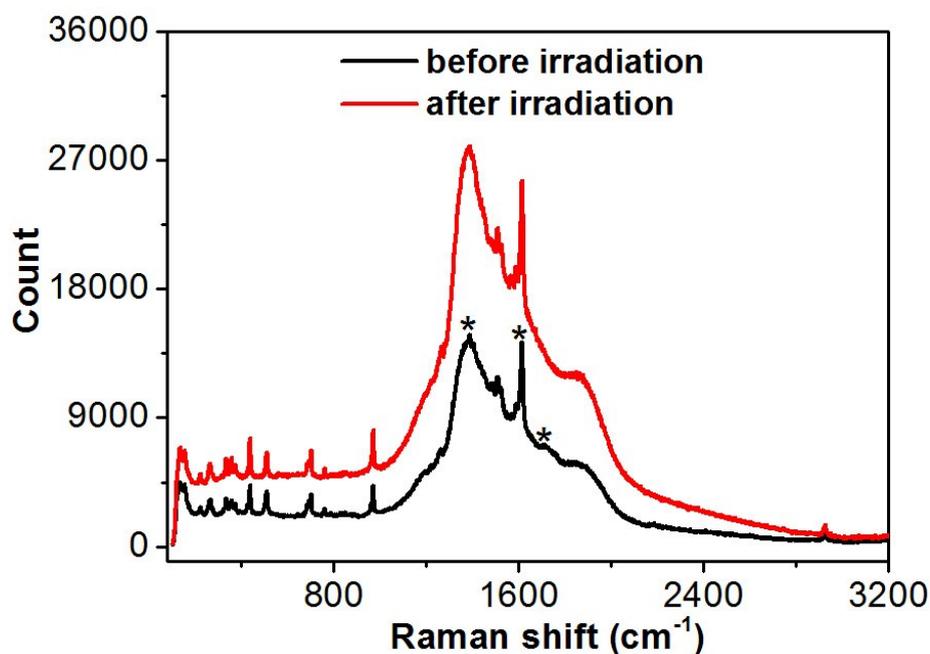

Fig. S5 The packing structure of **1**.
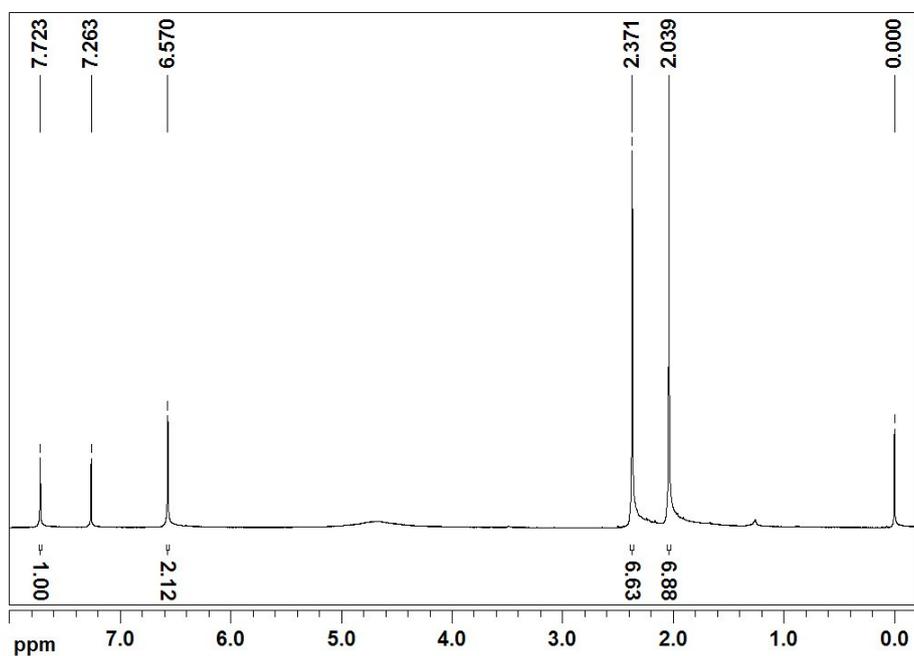

Fig. S6 The packing structure of **2**.

Fig. S7 Plots a and b: irradiating (λ = 365 nm) **1** for 0, 30 minutes, respectively; plots c and d: using 574 nm light to irradiate the sample corresponding to plot b for 10 and 20 minutes, respectively; plot e: placing the sample corresponding to plot b in the dark for 45 minutes.

Fig. S8 Raman spectra of **1** before and after irradiation (λ = 365 nm, 30 minutes), using laser light of 785 nm. Three peaks with * are at 1399, 1614 and 1711 cm^{-1}, respectively.
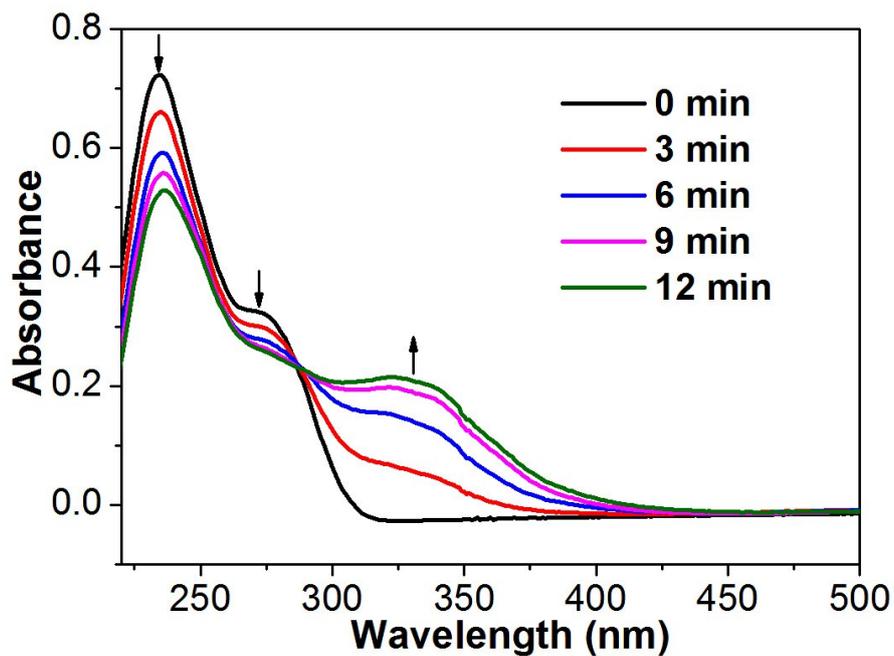
Fig. S9 Absorption spectra changes of **1** in CH$_3$CN solution (c = 2.4 × 10^{-5} M) upon UV irradiation (λ = 270 nm) for 0 to 12 minutes.

Fig. S10 ^{1}H NMR spectrum of **1** (500 MHz, CDCl$_3$) after UV irradiation (λ = 270 nm).

Fig. S11 ^{1}H NMR spectra of **1** before and after UV irradiation (λ = 270 nm).

Fig. S12 Plots a and b: irradiating (λ = 365 nm) **2** for 0, 20 minutes, respectively; plots c and d: using 624 nm light to irradiate the sample corresponding to plot b for 10 and 20 minutes, respectively; plot e: placing the sample corresponding to plot b in the dark for 40 minutes.
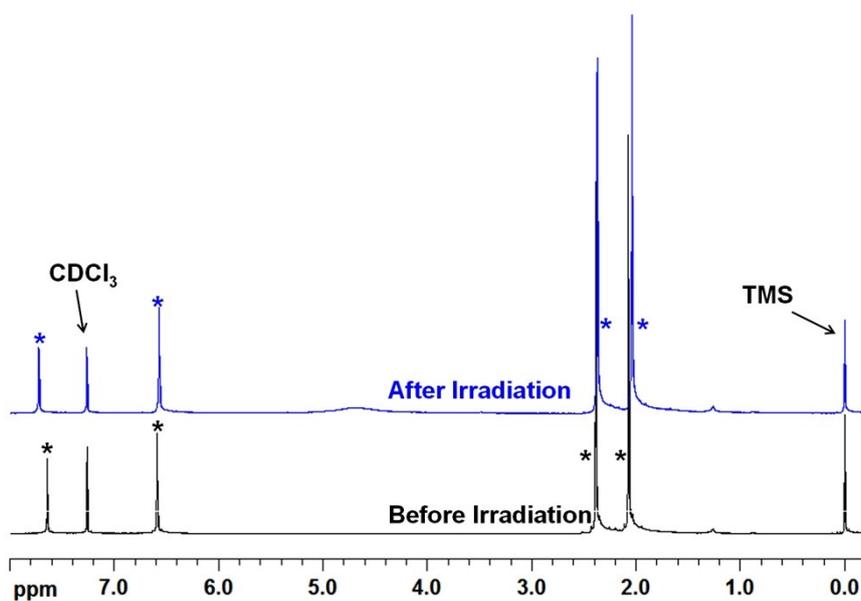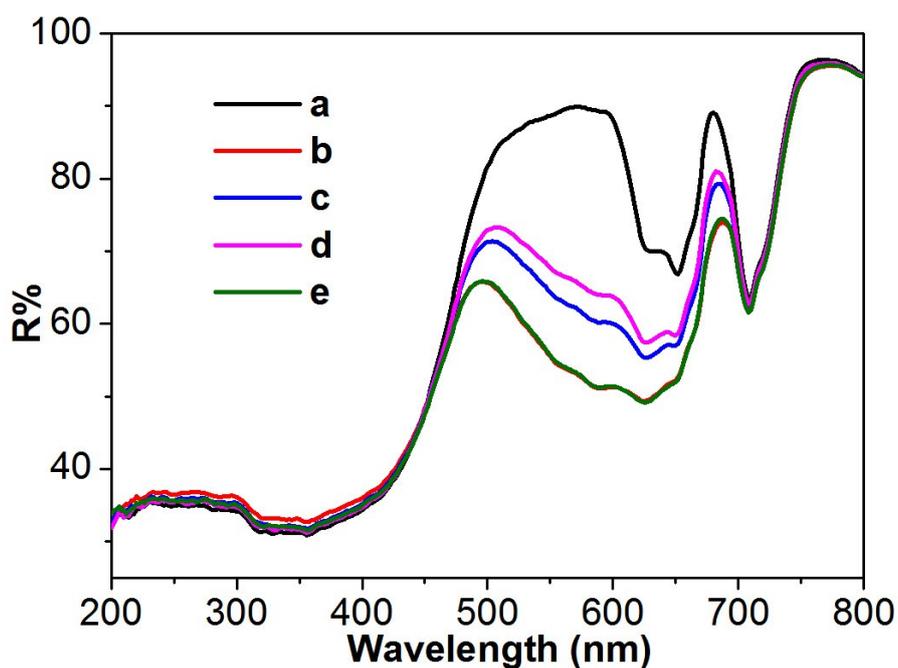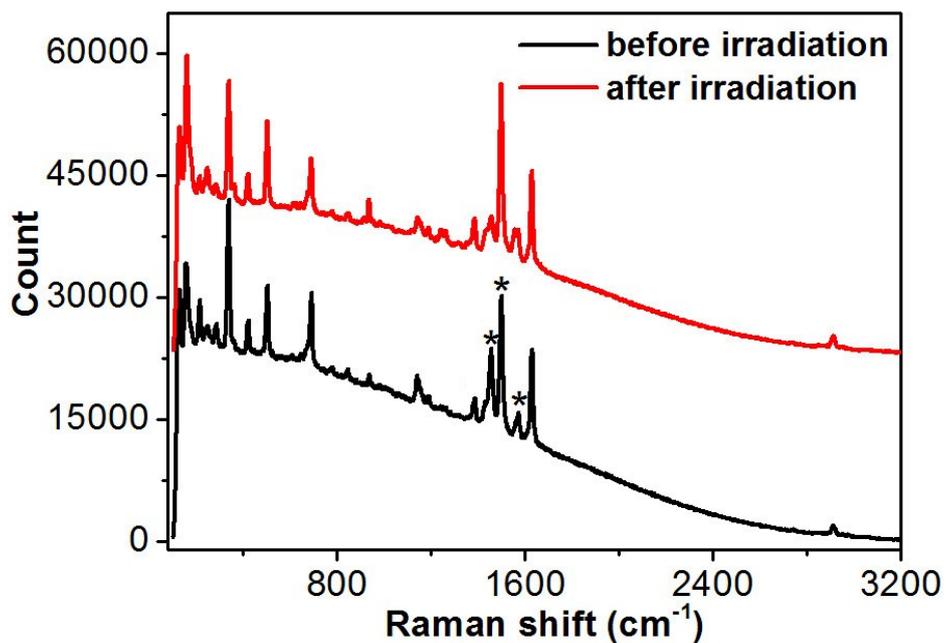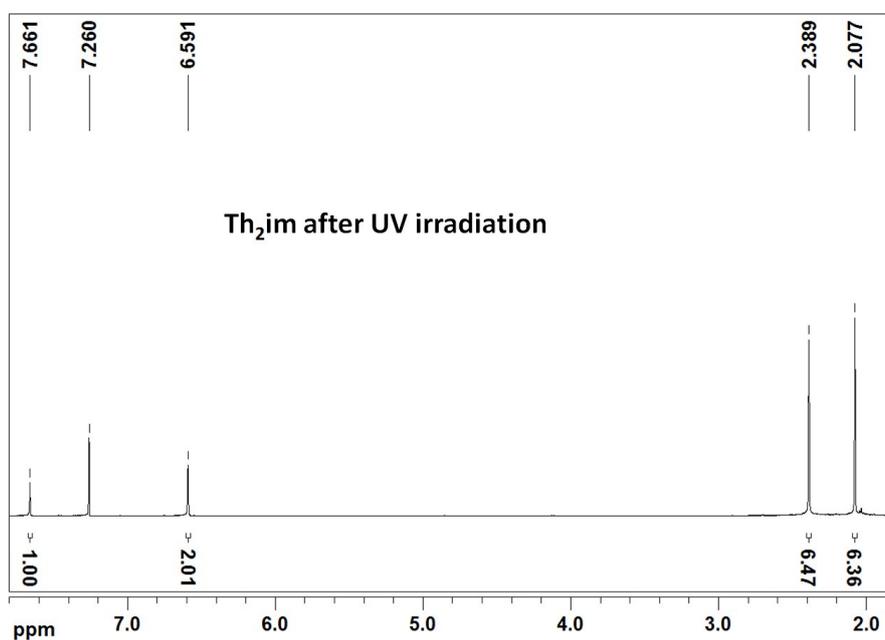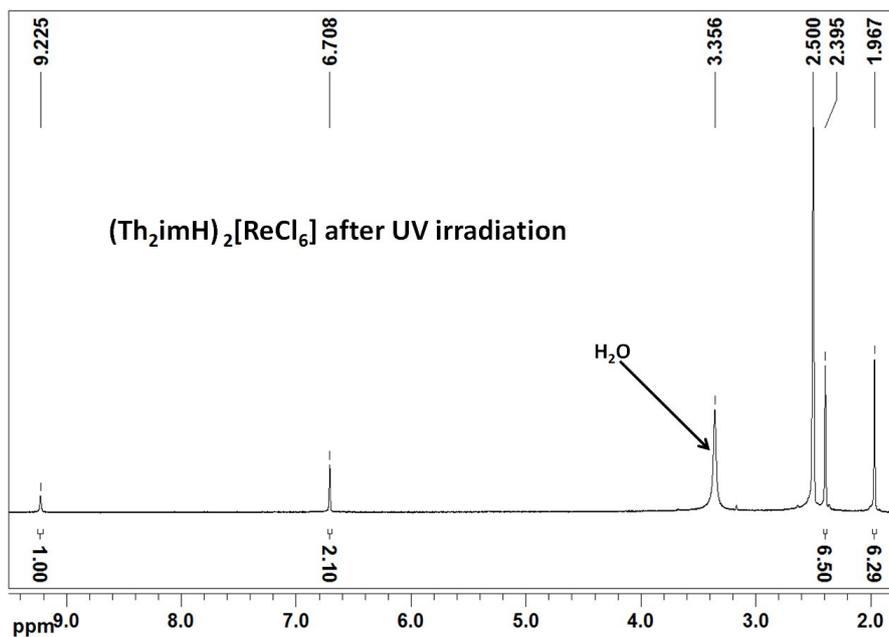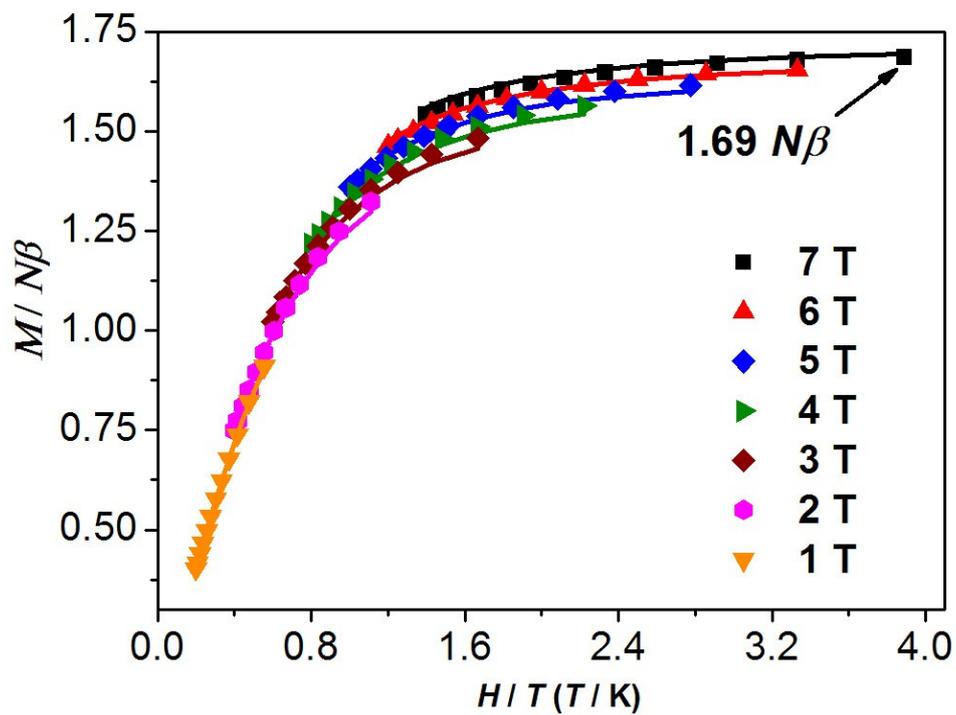
Fig. S13 Raman spectra of **2** before and after irradiation (λ = 365 nm, 20 minutes), using laser light of 785 nm. Three peaks with * are at 1457, 1500 and 1573 cm^{-1}, respectively.
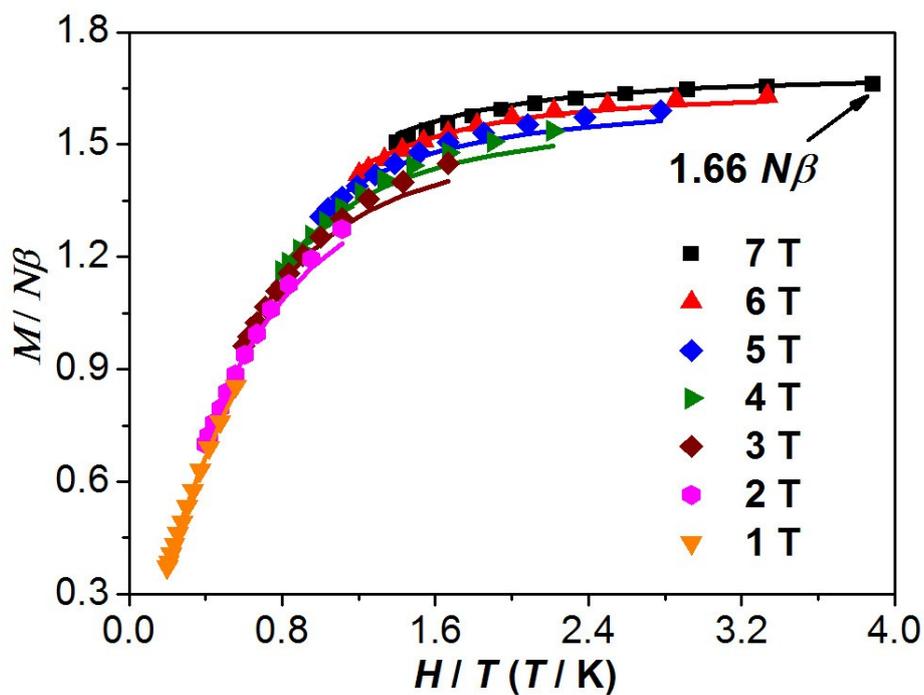

Fig. S14 ^{1}H NMR spectrum of the irradiated sample of **1** (500 MHz, CDCl$_3$; UV irradiation, λ = 365 nm).
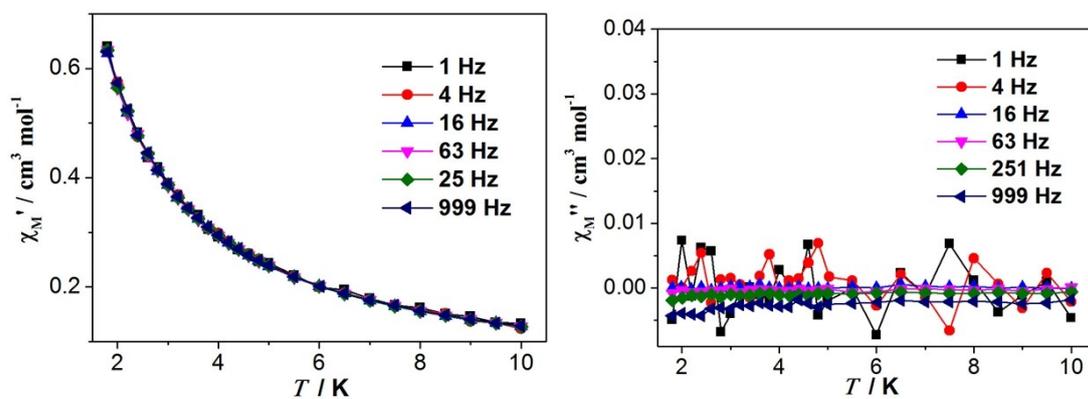
Fig. S15 ^{1}H NMR spectrum of the irradiated sample of **2** (500 MHz, DMSO-d_6; UV irradiation, λ = 365 nm).


Fig. S16 Low-temperature magnetization data for **2** collected under various applied dc fields. The solid lines represent fits to the data.

Fig. S17 Low-temperature magnetization data for **2L** collected under various applied dc fields. The solid lines represent fits to the data.
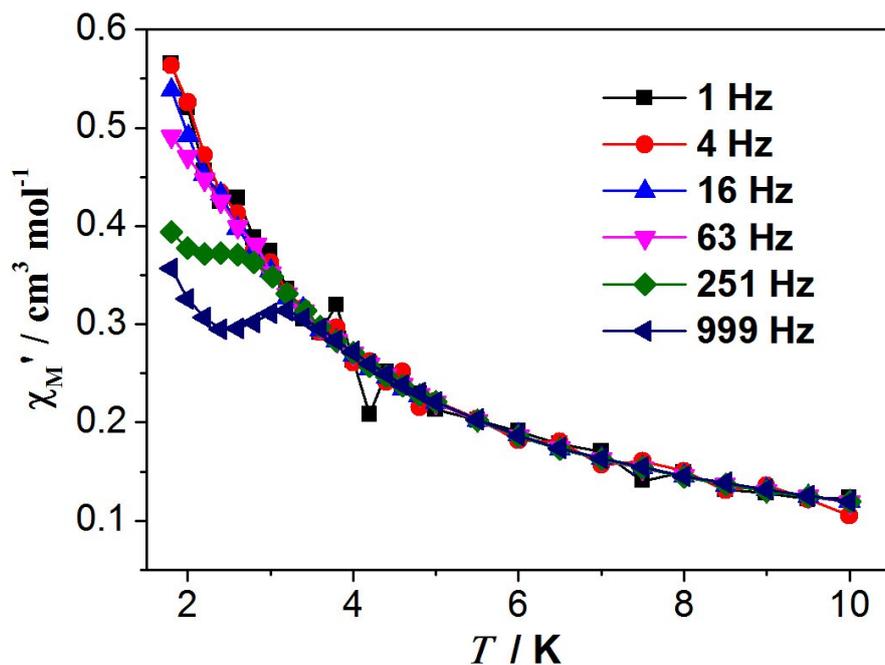

Fig. S18 Temperature dependence of ac susceptibilities of in-phase χ_M' (left) and out-of-phase χ_M" (right) for **2** under zero applied static field.
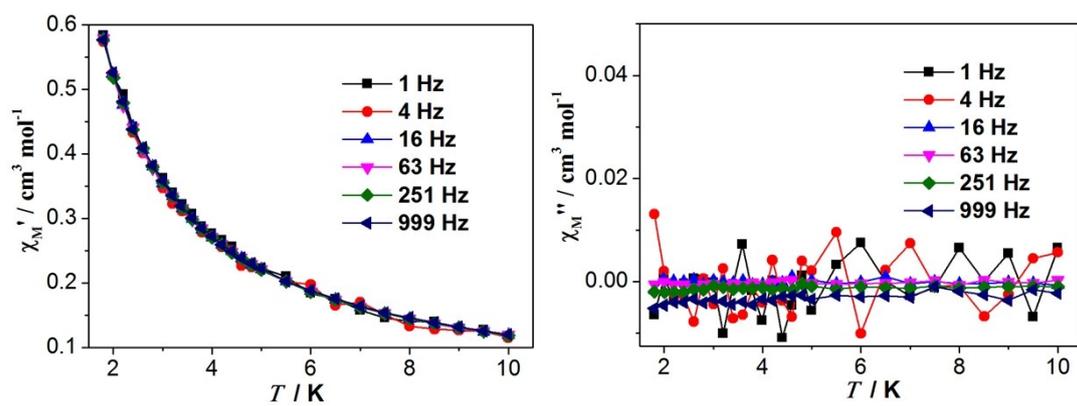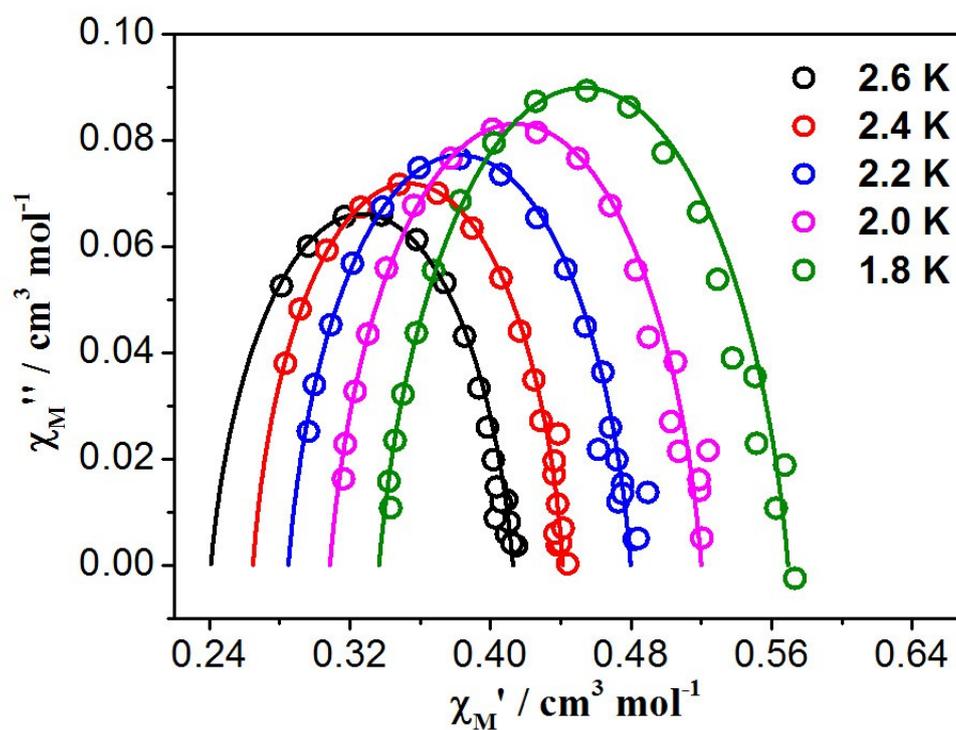
Fig. S19 Temperature dependence of ac susceptibilities of in-phase χ_M' (left) and out-of-phase χ_M'' (right) for **2L** under zero applied static field.
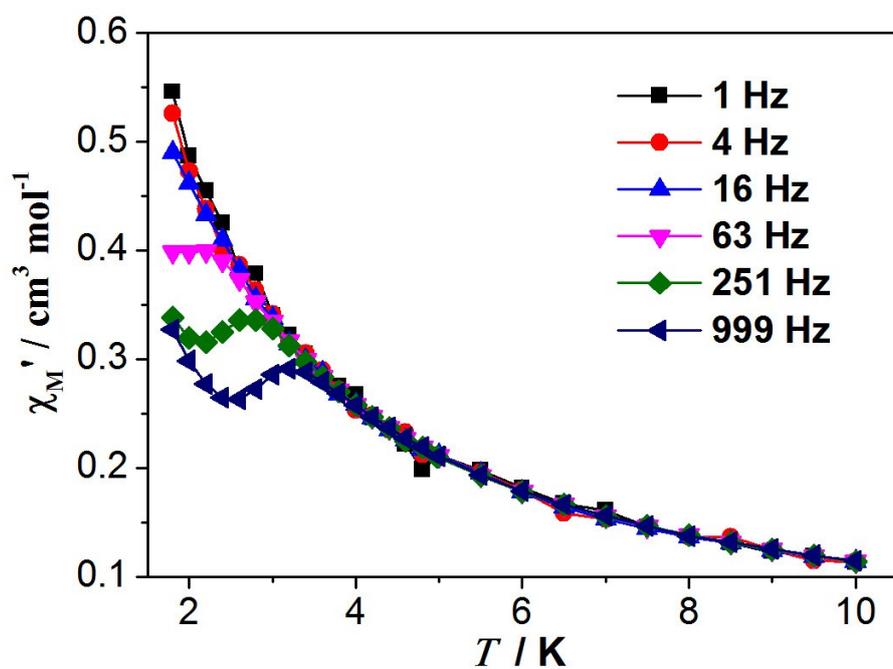

Fig. S20 Temperature dependence of ac susceptibilities of in-phase χ_M' for **2** under 1000 Oe applied static field.

Fig. S21 Temperature dependence of ac susceptibilities of in-phase χ_M' for **2L** under 1000 Oe applied static field.

Fig. S22 Cole-Cole plots of **2** in the temperature range of 1.8-2.6 K under applied static field of 1000 Oe; the solid lines are the best fit by Debye model ($\alpha < 0.17$).
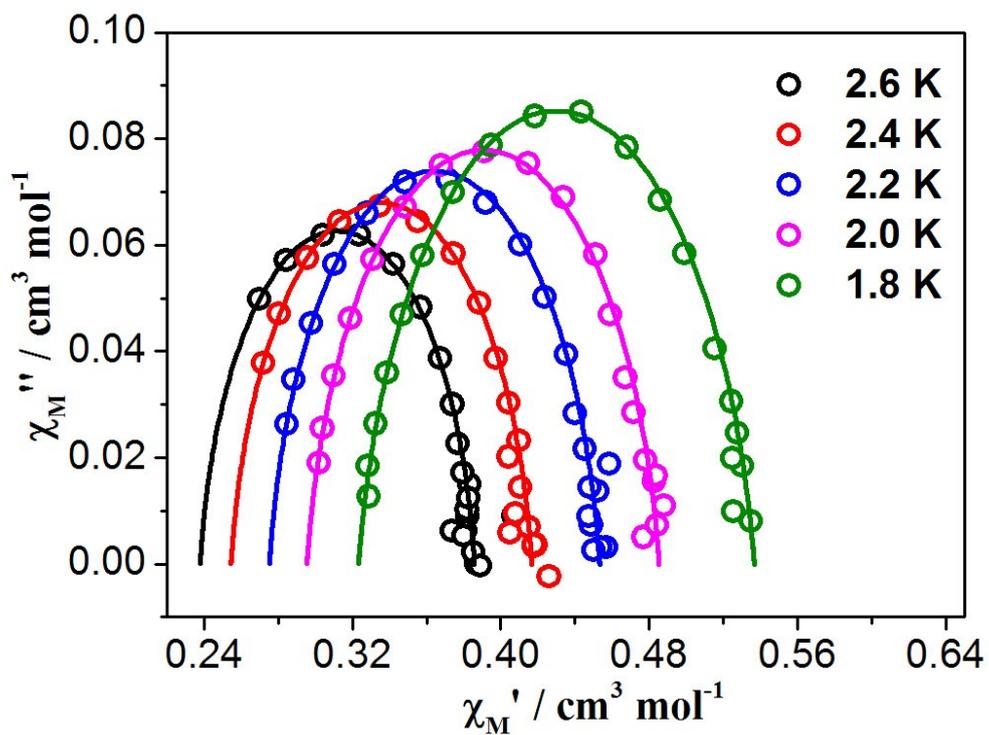
Fig. S23 Cole-Cole plots of **2L** in the temperature range of 1.8-2.6 K under applied static field of 1000 Oe; the solid lines are the best fit by Debye model ($\alpha < 0.14$).